

2011

# Drag Reduction of a Modern Straight Truck

Drew Landman

*Old Dominion University*, [dlandman@odu.edu](mailto:dlandman@odu.edu)

Matthew Cragun


*Old Dominion University*

Mike McCormick

*Old Dominion University*

Richard Wood

Follow this and additional works at: [https://digitalcommons.odu.edu/mae\\_fac\\_pubs](https://digitalcommons.odu.edu/mae_fac_pubs)

 Part of the [Aerodynamics and Fluid Mechanics Commons](#), [Automotive Engineering Commons](#), and the [Probability Commons](#)

## Repository Citation

Landman, Drew; Cragun, Matthew; McCormick, Mike; and Wood, Richard, "Drag Reduction of a Modern Straight Truck" (2011). *Mechanical & Aerospace Engineering Faculty Publications*. 37.  
[https://digitalcommons.odu.edu/mae\\_fac\\_pubs/37](https://digitalcommons.odu.edu/mae_fac_pubs/37)

## Original Publication Citation

Landman, D., Cragun, M., McCormick, M., & Wood, R. (2011). Drag reduction of a modern straight truck. *SAE International Journal of Commercial Vehicles*, 4(1), 256-262. doi:10.4271/2011-01-2283

## Drag Reduction of a Modern Straight Truck

2011-01-2283

Published  
09/13/2011Drew Landman, Matthew Cragun and Mike McCormick  
Old Dominion UnivRichard Wood  
Solus-Solutions and Technologies

Copyright © 2011 SAE International

doi:10.4271/2011-01-2283

### ABSTRACT

A wind tunnel test program was conducted at the Langley Full Scale Tunnel (LFST) to evaluate the performance of five passive drag reduction configurations on a modern straight truck at full scale. Configurations were tested in a build-up fashion with results representing a cumulative effect. Tested configurations include a front valance, a front box fairing, a boat-tail, an ideal side-skirt, and a practical side-skirt. Configurations were evaluated over a nominal 9 degree yaw sweep to establish wind averaged drag coefficients using SAE J1252. Genuine replicate yaw sweeps were used in an uncertainty analysis. Results show up to 28% improvement in wind-averaged drag coefficient and that significant gains can be made in straight truck fuel economy, even at non-highway speeds.

### INTRODUCTION

Aerodynamic performance in commercial trucks is becoming increasingly more important due to fuel costs as well as pressures due to environmental concerns. Currently the literature primarily contains information on the aerodynamic performance of larger tractor-trailer (class 8) vehicles, however, light and medium straight trucks (class 2-5) have relatively little available data by comparison-particularly using modern designs. This data is important not only because it provides an incentive to update vehicle fleets to improve performance, but also serves as a check of performance claims by makers of after-market components and devices for these vehicles. The latter is becoming more important as more products are entering the market-many of which make claims not substantiated by adequate testing.

Research was conducted at the Langley Full Scale Tunnel (shown in [Figure 1](#)) to evaluate the performance of several add-on devices using a full-scale modern straight truck. This work is aimed at contributing to the art by providing a data set with the following attributes:

- Ideal limits to popular device performance
- Modern vehicle design
- Full-scale vehicle
- Drag reduction devices representative of many current market offerings
- Minimal boundary effects over yaw sweep
- Sufficient Reynolds number
- Minimum interference from support structure
- Overall uncertainty analysis, (not back to back point repeatability)

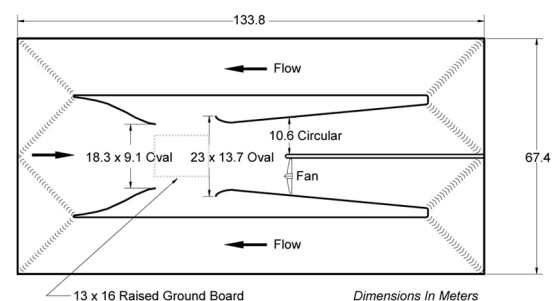


**Figure 1. The Langley Full Scale Tunnel Plan View**

## EVOLUTION OF HEAVY TRUCK DRAG REDUCTION TECHNOLOGIES

Drag reduction of commercial trucks has been explored since the 1930's with most of the focus, especially in recent years, on the tractor portion of class 8 vehicles.<sup>1,2,3,4</sup> Much of this work has application to light and medium straight trucks. The most recent work specific to straight trucks includes work done in the 1970's and 1980's--much of it by Cooper. Preliminary work included adding treatments above the cab to deflect air over the top of the box<sup>5</sup>. The later studies involved boat-tail designs at the rear of the vehicle<sup>6</sup>. These studies agree well with more general guidelines for vehicle development found in [reference 7](#). Additional details on advances in heavy truck aerodynamics can be found in [reference 8](#).

## EXPERIMENT DETAILS

### FACILITY

While operational, the LFST (formerly the NASA LaRC Full-Scale or NASA 30 by 60) featured a large  $\frac{3}{4}$  open-jet test section and large ground board.<sup>9</sup> Full-scale vehicles ranging from conventional cars to Class-8 tractors with shortened trailers could be accommodated. The test section was semi-elliptical in cross section with a width of 18.3 m (60 ft) and a height of 9.1 m (30 ft). The ground board measured 13 m wide by 16.0 m long and featured a turntable with a diameter of 8.7 m. The overall aerodynamic layout of the facility, used a double return design and is shown in [Figure 1](#). Power was supplied by two 3 MW (4000 HP) electric motors driving two 10.6 m diameter four-bladed fans. For this test the 6-DOF external balance with heavy truck supports was used to measure body-axis vehicle drag, side force, and yawing moment. Ground board boundary layer control was provided through a raised ground board.<sup>9</sup> The large  $\frac{3}{4}$  open jet test section of the LFST was well-suited to testing the full-size straight truck.

### VEHICLE

The vehicle used for testing was a full-size GMC T-series straight truck as shown in [Figure 2](#). The truck features a modern cab-forward design and a standard 16-foot box with radiused corners and edges.

Additionally, it should be noted that the vehicle includes a lift-gate at the rear of the vehicle.



*Figure 2. GMC T-series truck*

## DRAG REDUCTION DEVICES

Several devices were chosen for this test including a front valance, a fairing for the front of the box, a boat-tail at the rear of the box, an ideal side skirt, and a practical side skirt. All of these devices have been shown to be valid methods for reducing drag on ground vehicles, and a few are currently commercially available. The devices were tested in a “build-up” methodology where treatments were progressively added to the vehicle. [Figure 3](#) shows the vehicle treatments. [Figure 4](#) shows the progressive build-up of devices.

### Valance

A valance was added at the front of the vehicle at the front bumper. The valance extended from the bumper down to 3” from the ground and wrapped around the sides to the front wheel well openings. Adding a valance to restrict flow to high drag underbody components is a well known practice among other ground vehicles.

### Box Treatment

A commercially available product design to fair the front of the cargo box was added. Streamlining the box has been used as a means of drag reduction for the past 35 years. This helps to reduce the stagnation zone on the front of the box and reduce separation on the sides and top surfaces.

### Frame Extension Boat-tail

A patented boat-tail concept ([ref A](#)) was added at the rear of the vehicle to aid in base pressure recovery. The boat tail was added on three sides with the freight box floor aft platform acting as the fourth side. The boat-tail consisted of a 18 in. frame extension tapered at 15 degrees from the roof and sides of the box.

### Practical Skirt

The patent pending practical skirt is designed to restrict under body flow impingement onto high-drag undercarriage components--particularly at yaw conditions. The practical side-skirts extended from the lower surface of the freight box to 8 in. above the ground. The skirt extends longitudinally the

full length of the freight box. The forward most section of the skirt is curved inward to form an air dam. Because of the inset rear wheels of this truck's design, the skirt covered the wheels as well with no interference.

#### Ideal Skirt

The patent-pending ideal skirt is similar to the practical skirt except ground clearance is reduced to 3 in. Although it is impractical for regular use as a rigid panel, it serves to bound the ideal limits of performance

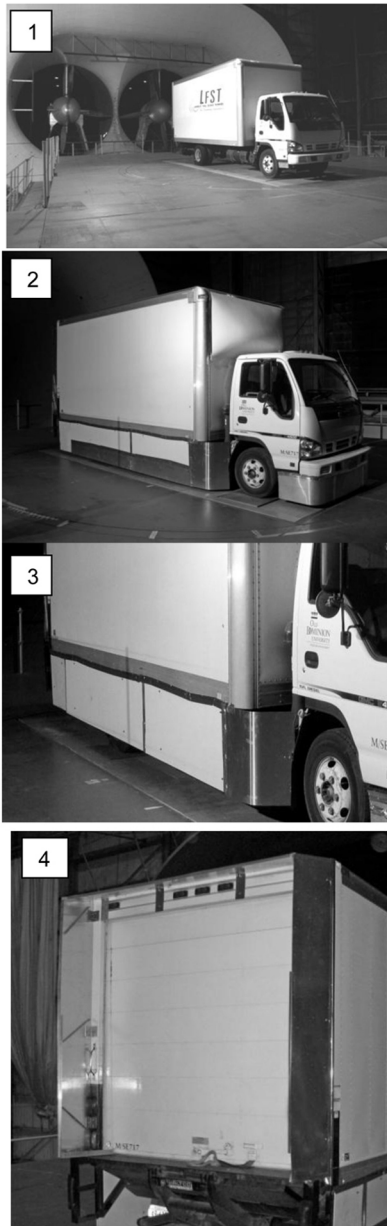


**Figure 3. Treatments for Box Truck: 1--Untreated truck on ground board. 2--Truck shown with valance, box front treatment, and 'ideal' skirt. 3--Truck shown with 'practical' skirt. 4--Truck shown with boat-tail.**

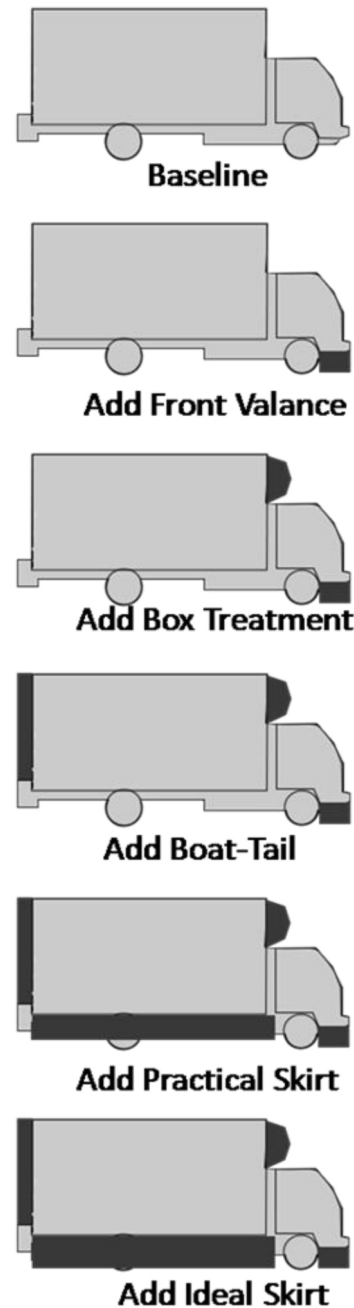


**Figure 4. Test Configurations**

### Test Procedure and Data Reduction

#### Test Conditions and Drag Measurement

All configurations were tested at a nominal dynamic pressure of 10 psf over a yaw sweep of 0 to 9 degrees with data to 15 degrees for the baseline case. Two of the configurations were chosen at random to be run as replicates for uncertainty estimates. A PC-based data acquisition system with a 16-bit A/D samples automotive balance load cell forces as well as a differential pressure transducer dedicated to dynamic pressure measurement. The drag force measurement and wind tunnel

dynamic pressure calibration was conducted as specified in the SAE J1252 recommended practice. Detailed data for each configuration yaw sweep is presented in the summary plot of [Figure 6](#).

#### Response Model

A cubic spline was fit to each configuration yaw sweep to allow interpolation between the recorded yaw values and those required for calculation of wind averaged drag coefficients at various highway speeds.<sup>11</sup> Wind averaged drag coefficients calculated using the method described in SAE J1252 with a chosen highway speed of 35 and 55 were calculated. Performance for components in a build-up methodology are shown in [Table 1](#) (55 mph) and [Table 2](#) (35mph). A sample spline fit is shown in [Figure 5](#).

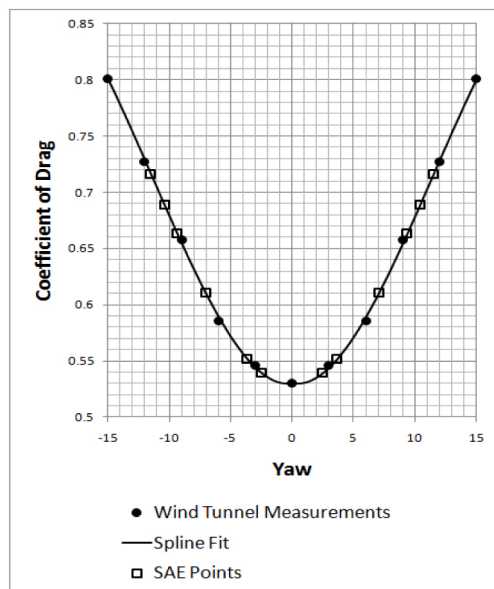


**Figure 5. Sample Cubic Spline Fit (Example data only - not from current test)**

#### Uncertainty Analysis

An uncertainty estimate (U) for an individual drag coefficient measurement was obtained by combining bias (B) and true precision (P) errors.<sup>12</sup>

$$U^2 = B^2 + P^2$$

1)

This procedure was first presented in [reference 1](#). The precision error is the random error component that is best obtained by the replication of measurements of the desired response. In this experiment two pairs of replicate runs were performed allowing a sum of squares of differences to be computed between the pairs. A true replicate requires that a given configuration run is conducted, subsequent runs follow which require changes in the geometry (preferably in random

order), and then the replicated run is conducted later in the test program. This insures that the precision estimate includes the error associated with removing and replacing the devices on the model.<sup>13</sup> Many authors use repeat runs (no geometry change) for precision estimation which by nature results in lower precision estimates. The replicate based precision measurement is then an honest estimate of the true uncertainty associated with not only measuring the flow conditions and forces, but also the ability to control the model geometry. Measured drag coefficients from two replicate runs were used to provide an estimate of the variance

**Table 1. Component Drag Reductions from Baseline at 55 mph**

Configuration	$C_{D_{wavg}}$	$\Delta C_{D_{wavg}}$	% Change
Baseline	0.582	0	0.0
Add Valence	0.552	0.03	5.2
Add cargo box front treat	0.538	0.044	7.6
Add boat tail	0.518	0.064	11.0
Add practical side skirt	0.466	0.116	19.9
Add ideal side skirt	0.448	0.134	23.0

**Table 2. Component Drag Reduction from Baseline at 35 mph**

Configuration	$C_{D_{wavg}}$	$\Delta C_{D_{wavg}}$	% Change
Baseline	0.659	0	0.0
Add Valence	0.654	0.005	0.8
Add cargo box front treat	0.612	0.047	7.1
Add boat tail	0.587	0.072	10.9
Add practical side skirt	0.486	0.173	26.3
Add ideal side skirt	0.472	0.187	28.4

Using the two pairs of runs, the variance may be pooled to give a single value representative of the entire test.

To calculate the variance ( $S^2$ ) associated with a pair of replicate runs, the quotient is formed by the root sum square of differences for the  $n$  runs over the degrees of freedom (number of runs less one):<sup>13</sup>

$$S^2 = \frac{\sum_{i=1}^n (C_{D_{1i}} - C_{D_{2i}})^2}{n-1} \quad (2)$$

In [equation 2](#),  $C_{D1}$  represents a drag coefficient value at the  $i$ th yaw angle from the initial run and  $C_{D2}$  the replicate at the same yaw angle. Set point error between the points may be adjusted out by using a fitted response function such as the cubic spline. To pool the variances of two pairs of replicate runs, the number of degrees of freedom are used as weights:<sup>14</sup>



$$S_p^2 = \frac{(n_1 - 1)S_1^2 + (n_2 - 1)S_2^2}{n_1 + n_2 - 2} \quad (3)$$

The precision, P for a single measurement of the mean drag coefficient is found by including a coverage factor for the desired confidence level (t statistic) with the estimate of the standard deviation.<sup>12,14</sup> There were a total of N= 8 replicated values from two configurations which were pooled for the variance estimate. For a 95% confidence interval, the precision may be expressed as:

$$P = \frac{2S_p}{\sqrt{N}} \quad (4)$$

The bias error in this experiment is the systematic error due to the instrumentation. The bias estimates can be found through the data reduction equation used to calculate the drag coefficient. If D is the measured drag force, q the measured dynamic pressure, and A the vehicle frontal area then  $C_D$  is:

$$C_D = \frac{D}{qA} \quad (5)$$

Using the method of [reference 12](#), holding frontal area constant, the bias may be expressed as:

$$B^2 = \left[ \frac{\partial C_D}{\partial D} B_D \right]^2 + \left[ \frac{\partial C_D}{\partial q} B_q \right]^2 \quad (6)$$

Performing the partial differentiations:

$$B^2 = \left[ \frac{1}{qA} B_D \right]^2 + \left[ \frac{-D}{q^2 A} B_q \right]^2 \quad (7)$$

Over the range  $0.3 < C_D < 0.6$ , the estimated uncertainty in obtaining a mean value for drag coefficient at a single yaw value is  $\pm 0.003$  with 95% confidence.

## DISCUSSION OF RESULTS

[Figure 6](#) shows the performance of the vehicle over a range of yaw conditions as the devices were added in a progressive build up. The untreated truck shows non-linear behavior with body-axis drag increasing significantly as yaw is increased. The addition of the valance has noticeable impact in low-yaw conditions, but performance degrades over the yaw sweep even faster than the baseline case.

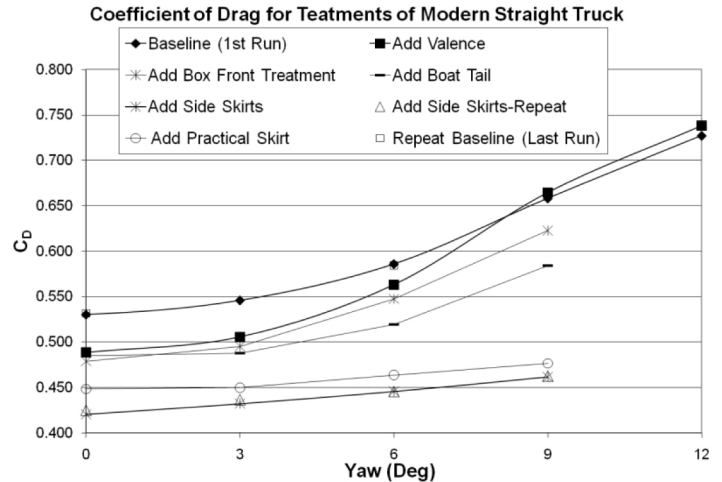


**Figure 6. Detailed Configuration Yaw Sweep Data Summary**

As the device build-up progresses, the drag dependency on yaw assumes a more linear character. In reviewing the yaw sweeps of [Figure 6](#), it can be seen that the overall trend in the drag response with yaw for each of the devices compares favorably to that shown in [references 4,5, and 15](#). As the cross-flows under the body are blocked, body-axis drag increases are significantly reduced with increasing yaw. In the limit, the fully treated truck body-axis drag is relatively insensitive to yaw changes.

[Figure 7](#) shows the incremental percent change in performance of the wind-averaged values of the data seen in [Figure 6](#). In these plots, it is easy to see that the addition of side skirts yielded the greatest impact on the wind averaged drag coefficient. The two skirt configurations chosen for this study were meant to show both the maximum body-axis drag reduction available from the addition of a skirt, but also a more conservative, “realistic” design that could be used in daily service. Illustrating both configurations is important for two reasons: first, having a value for an ‘ideal’ skirt demonstrates the maximum potential performance gain available by the addition of side-skirts. Second, this demonstrates that the tradeoff between an ‘ideal’ skirt and ‘realistic’ one is one of diminishing returns and the ‘realistic’ skirt offers a near ‘ideal’ benefit. Further gains may be made using a rigid practical length skirt with flexible extensions. The skirts are especially effective at lower speeds. At lower speeds, the cross-wind velocity is proportionally much larger in the wind-average than at higher speeds; because of this, the reduced yaw sensitivity of the skirts is very advantageous.

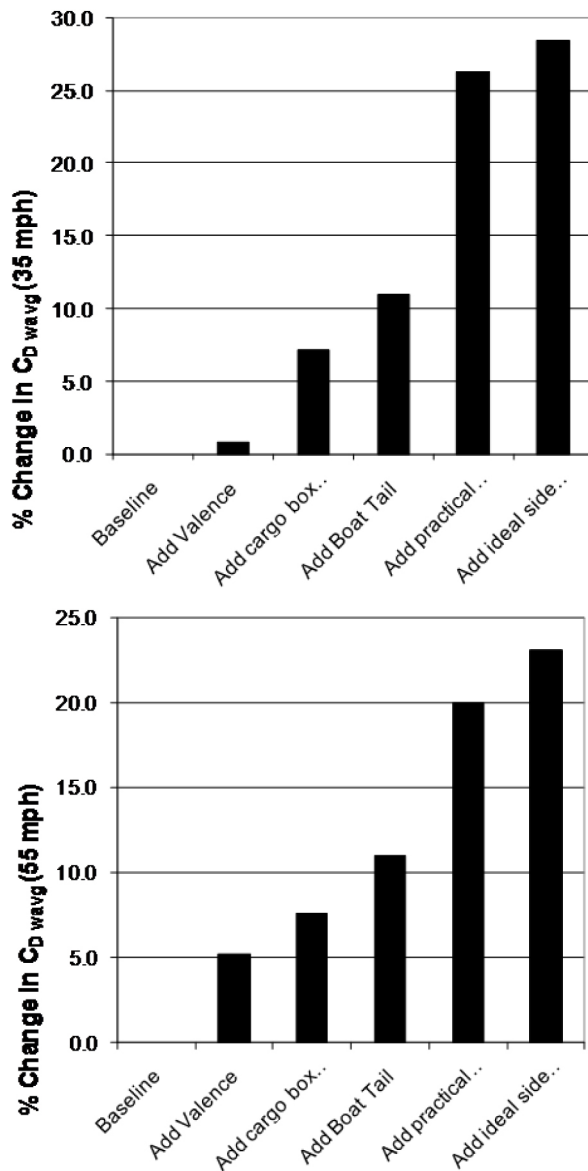


Figure 7. Change in Wind Averaged Drag Coefficients

With regards to the valance, the greatest gains are realized in a low-yaw condition. As yaw increases, the performance is degraded presumably due to ingress of flow through the wheel well/valance gap. When the wind-average is taken, particularly at a low velocity, the gains are very small. The wind-averaged gain is larger at higher vehicle velocity conditions when the relative cross-wind velocity becomes proportionally smaller in the wind-averaging scheme. Careful tailoring of the valance and front wheel well/fender section should alleviate the yaw sensitivity.

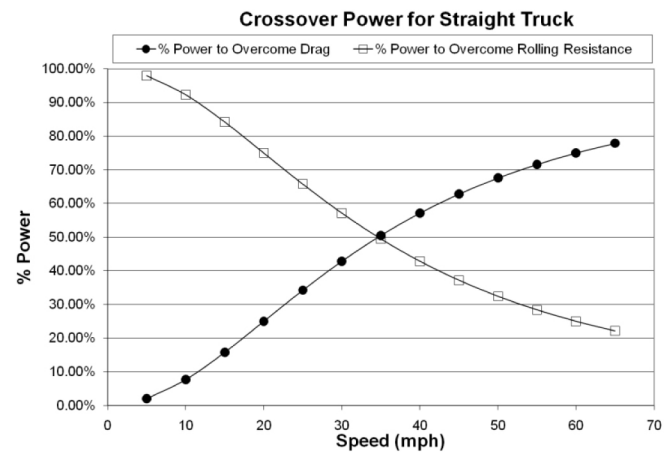


Figure 8. Crossover power for a straight truck

The impact of the front cargo box treatment is also of note as several devices of this nature are on the market today. Work has been done on similar treatments as early as the 1970's.<sup>5</sup> Early tests showed significant reductions in drag. However, drag reductions in this test, appear to be much more modest. One explanation for this is the shape of the box on a modern truck. The boxes on modern trucks have radiused corners, whereas earlier models, similar to the ones used in earlier testing had square corners with the associated large scale separations.<sup>6,7</sup> Modern straight trucks, such as the model used here, also feature more streamlined cab designs with features such as radiused corners, raked wind shields, and tapered sides which all serve to condition the flow onto the box.

Of importance in this study is the data included for the relatively low speed of 35mph. In contrast to a larger tractor-trailer combination which operates in long-haul scenarios at highway speeds, box trucks typically operate in a smaller service area and at reduced speeds. By converting the body-axis drag into power at different velocities and comparing that to rolling resistance, a plot of cross-over power can be made. For this study, a typical coefficient of rolling resistance of 0.01 was used along with an assumed vehicle weight of 10,000 lbs. Looking at the plot of cross-over as shown in Figure 8, it can be seen that the aerodynamic forces begin to become dominant around 35 mph. This illustrates that drag reduction, even at more modest speeds and for lighter vehicles, is a viable means of improving efficiency.

## CONCLUSION

As drag reduction devices gain greater acceptance and use on heavy trucks as a viable means of improving fuel economy and reducing emissions, it is important that proper attention be paid to light and medium straight trucks as well. The results of these studies show that gains for commercial straight trucks traveling at less than highway speed are still of

significant value and techniques similar to those used on heavy trucks may be employed on light and medium straight trucks. It is the hope of the authors that this work will add to prior art by providing a data set on a modern straight truck. This data may be useful from both a design perspective and as check against various commercial claims for improvements offered by the aftermarket industry.

Additionally, the uncertainty analysis provided in this study is offered as an more rigorous assessment of measurement error. As the incremental aerodynamic improvements become smaller, an understanding of the uncertainty is critical to understanding a device's significance, and consequently its value.

## REFERENCES

1. Landman, D., Wood, R., Seay, W., and Bledsoe, J., "Understanding Practical Limits to Heavy Truck Drag Reduction," *SAE Int. J. Commer. Veh.* **2**(2):183-190, 2010, doi:[10.4271/2009-01-2890](https://doi.org/10.4271/2009-01-2890).
2. Wood, R., "Operationally-Practical & Aerodynamically-Robust Heavy Truck Trailer Drag Reduction Technology," *SAE Int. J. Commer. Veh.* **1**(1):237-247, 2009, doi:[10.4271/2008-01-2603](https://doi.org/10.4271/2008-01-2603).
3. Schoon, R. and Pan, F., "Practical Devices for Heavy Truck Aerodynamic Drag Reduction," SAE Technical Paper [2007-01-1781](https://doi.org/10.4271/2007-01-1781), 2007, doi:[10.4271/2007-01-1781](https://doi.org/10.4271/2007-01-1781).
4. Leuschen, J. and Cooper, K., "Full-Scale Wind Tunnel Tests of Production and Prototype, Second-Generation Aerodynamic Drag-Reducing Devices for Tractor-Trailers," SAE Technical Paper [2006-01-3456](https://doi.org/10.4271/2006-01-3456), 2006, doi:[10.4271/2006-01-3456](https://doi.org/10.4271/2006-01-3456).
5. Cooper, K.R., "A Wind Tunnel Investigation into the Fuel Savings Available from the Aerodynamic Drag Reduction of Trucks." DME/NAE Quarterly Bulletin No. 1976(3), 1976
6. Cooper, K., "The Effect of Front-Edge Rounding and Rear-Edge Shaping on the Aerodynamic Drag of Bluff Vehicles in Ground Proximity," SAE Technical Paper [850288](https://doi.org/10.4271/850288), 1985, doi: [10.4271/850288](https://doi.org/10.4271/850288).
7. Hucho, W.-H., "Aerodynamics of Road Vehicles," SAE International, Warrendale, PA, ISBN 978-0-7680-0029-0, 1998.
8. McCallen, R. et al. (ed.), "The Aerodynamics of Heavy Vehicles: Trucks, Buses, and Trains," *Lecture Notes in Applied Computational Mechanics*, V 19, pp 9-28, Springer, 2002
9. Landman, D. and Britcher, C., "Development of Race Car Testing at the Langley Full-Scale Tunnel," SAE Technical Paper [983040](https://doi.org/10.4271/983040), 1998, doi: [10.4271/983040](https://doi.org/10.4271/983040).
10. Landman, D., et al. "A Study of Ground Simulation for Wind Tunnel Testing of Full-Scale NASCAR's," AIAA paper

2000-153, presented at the 38th Aerospace Sciences Meeting and Exhibit, Reno, NV, January 10-13, 2000

11. Mathcad V12, [www.mathsoft.com](http://www.mathsoft.com)
12. Coleman, H. and Steele, G., *Experimental Uncertainty Analysis for Engineers*, 2<sup>nd</sup> ed., Wiley, 1999
13. Montgomery, D.C., *Design and Analysis of Experiments*, 7th ed., Wiley, 2008.
14. Montgomery, D.C. and Runger, "Applied Statistics and Probability for Engineers," 4th ed., Wiley, 2008
15. Cooper, K., "Truck Aerodynamics Reborn - Lessons from the Past," SAE Technical Paper [2003-01-3376](https://doi.org/10.4271/2003-01-3376), 2003, doi:[10.4271/2003-01-3376](https://doi.org/10.4271/2003-01-3376).

**Ref A.** Wood, R.; Frame extension device for reducing the aerodynamic drag of ground vehicles. USPTO 7585015

## CONTACT

Dr. Drew Landman is a Professor of Aerospace Engineering at Old Dominion University. Email: [dlandman@odu.edu](mailto:dlandman@odu.edu)

Mr. Mike McCormick was a student at Old Dominion University and is now an engineer at Disney. Email: [mccormick454@gmail.com](mailto:mccormick454@gmail.com)

Mr. Matthew Cragun was a student at Old Dominion University and is now an engineer at TotalSim US. Email: [mcragun@totalsim.us](mailto:mcragun@totalsim.us)

Mr. Richard Wood is president of SOLUS Solution and Technologies LLC. Email: [rick@solusinc.com](mailto:rick@solusinc.com)